GEOPHYSICAL RESEARCH LETTERS, VOL. 25, NO. 5, PAGES 713-716, MARCH 1, 1998

Current-Voltage characteristics of the tethered satellite system: Measurements and uncertainties due to temperature variations

C.L. Chang,[1] A.T. Drobot,[1] K. Papadopoulos,[1] K.H. Wright,[2] N.H. Stone,[3]
C. Gurgiolo,[4] J.D. Winningham,[5] and C. Bonifazi[6]

Abstract. One of the primary goals of the Tethered Satellite System reflight mission (TSS-1R) is to determine the current-voltage characteristics of the TSS satellite orbiting in the ionosphere. While the collected current was measured directly with high reliability, the satellite potential could only be deduced from a circuit model or from interpretation of measurement data below satellite potentials of 500 Volts. The greatest uncertainty in the circuit model is the value of tether resistance R. We have provided quantitative calibration of the resistance based on instrument data for Vs < 100 Volts. We have reached the important conclusion that the R value in the TSS circuit model is correlated to temperature changes associated with the diurnal cycles along the TSS flight path. We have also applied the calibrated R value in the TSS circuit equation to construct the I-V curves that extend to high voltages. The resulting I-V characteristics are presented with error bounds on satellite potential to indicate the uncertainty associated with the tether resistance determination. The I-V relation exhibits different scalings in the high (> 100 Volts) and low (< 10 Volts) voltage regimes, which indicates a fundamental transition for the current collection physics in the ionospheric plasma surrounding the satellite.

I-V Measurement of the TSS Satellite

A major objective of the TSS-1R mission was to determine the current-voltage (I-V) characteristics of the tethered satellite moving at the orbital velocity of the Low Earth Orbit (LEO) [*Stone and Bonifazi*, 1997]. The I-V characteristic was determined by a pre-programmed TSS science operation called the IV-24 operating cycle. During the IV-24 cycle, a current sequence was performed by stepping the command current delivered by the Electron Generator Assemblies (EGAs) in the payload bay of the Orbiter, thus modifying the satellite potential. A complete IV-24 cycle contains six repeating current sequences with each sequence lasting four minutes [*Dobrowolny and Stone*, 1994]. During the TSS-1R mission, three IV-24 cycles were completed. The first IV-24 cycle lasted from 056/23:20:30 to 056/23:44:30 UT in a day orbit. The second IV-24 cycle lasted from 057/00:12:00 to 057/00:36:00 UT in the subsequent night orbit. The last IV-24 cycle lasted from 057/01:06:00 to 057/01:30:00 UT in a day orbit.

During each of the command current pulses, the actual current I flowing through the tether is measured directly by the Tether Current and Voltage Monitor (TCVM) of the Shuttle Electrodynamics Tether System (SETS) investigation [*Aguero et al.*, 1994] and by the Satellite Ammeter (SA) of the Satellite Core Equipment (SCORE) investigation [*Bonifazi et al.*, 1994]. The satellite voltage Vs, defined by the potential difference between the satellite and the ionospheric plasma, can be deduced from the boom-mounted sensor package (BMSP) operated by the Research on Orbital Plasma Electrodynamics (ROPE) investigation [*Stone et al.*, 1994]. The BMSP records the current collected by the instruments located on the fixed boom (1 m in length) of the satellite. It is electrically isolated from the satellite and its potential is powered by the Floating Supply (FS), which links the BMSP to the satellite through a 700 KΩ resistance. The FS can bias the BMSP in the range of 0 to -500 Volts relative to the satellite in incremental voltage steps of 0.122 Volts. For satellite potentials up to 500 Volts, the FS is automatically adjusted to minimize the current collected by the BMSP, thus maintaining its potential near the local plasma potential. The potential adjustment made by FS to keep the BMSP at floating potential can be interpreted as the satellite potential, Vs, subject to a number of caveats regarding the electron distribution function. Operationally, the determination of satellite potential Vs is accomplished by a seek and track routine. In the seek mode, the FS bias voltage is adjusted in steps until the current collected by the BMSP approaches zero. Following the seek mode, the track routine is activated. Under this condition the FS bias voltage is fine-tuned continuously to keep the BMSP current around zero. The satellite potential relative to the ionospheric plasma is determined when the FS bias potential reaches a plateau. To ensure accurate readings of Vs, we took into account two practical considerations. First, the FS potential correction corresponds to the actual satellite potential provided that the BMSP is situated outside the sheath surrounding the satellite. Second, for large potentials the FS cannot step the bias potential fast enough to reach a plateau within the two seconds time period of the current pulse. Both of these considerations can be satisfied at low satellite potential. Therefore, we restrict ourselves to the Vs measurements in the range of 1 Volt < Vs < 100 Volts. The lower bound of Vs is set to be 1 Volt to ensure sufficient instrument sensitivity.

We took a two-step approach to construct the I-V curves for the entire range of the satellite potential. The first step is to calibrate the tether resistance R using the BMSP data of 1 Volt < Vs < 100 Volts. The second step is to compute Vs based on the calibrated R value and to impose error bounds based on the uncertainties associated with the statistical measurements. Both steps use the equivalent TSS circuit as shown in Figure 1. In this figure, Vs and Vo represent the potential drops across the plasma sheaths surrounding the satellite and the Orbiter. Correspondingly, Vg is the potential drop between the cathodes of the electron accelerators and the Orbiter body; I is the tether current and R is the overall dc resistance of the tether wire, which is approximately 2.1 KΩ at room temperature. Taking the motional induced EMF generated by a moving TSS-Orbiter system to be Ve, the TSS circuit equation can be expressed as

$$\mathrm{Ve} = \mathrm{Vs} + \mathrm{I\,R} + \mathrm{Vg} + \mathrm{Vo}\ . \tag{1}$$

To perform calibration in the first step, the tether resistance R is determined by substituting Vs and other directly measured quantities such as I, Ve, Vg, and Vo into Eq. (1). In the second step, a reverse process is taken, namely, using mean values of R and standard deviation ΔR in (1) to obtain Vs as a function of I.

Paper number 97GL02981.
0094-8534/98/97GL-02981$05.00

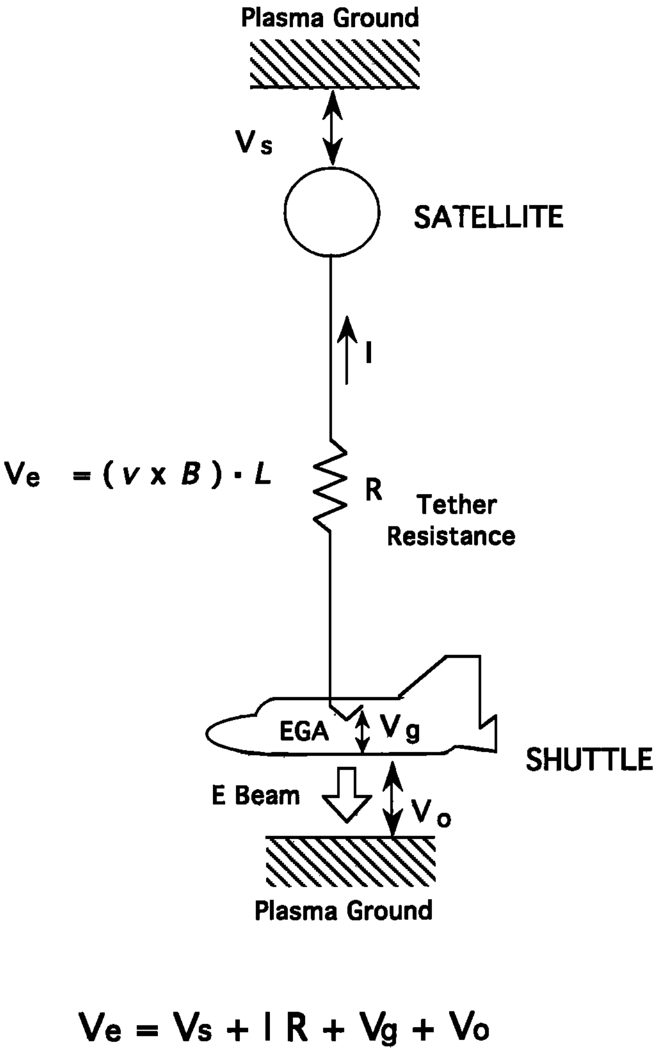

Figure 1. Schematic layout of the equivalent TSS circuit that corresponds to equation (1).

Temperature Dependent Tether Resistance

Direct measurements of various potential terms in (1) were performed by instruments onboard the Orbiter and the satellite during the TSS-1R mission. For instance, the Vg was measured by the voltmeter of the Deployer Core Equipment (DCORE-DV) [*Bonifazi et al.*, 1994] and by the Tether Current and Voltage Monitor (TCVM) of the Shuttle Electrodynamics Tether System (SETS) [*Aguero et al.*, 1994, *Thompson et al.*, 1997]. The Ve was measured by the TCVM and the DCORE-DV in between the current pulses when the EGAs were off and the current I=0. The Shuttle potential Vo, although not directly measured, was inferred from the Electrostatic Analyzers (ESAs) of the Shuttle Potential and Return Electron Experiment (SPREE) [*Oberhardt et al.*, 1994; *Burke et al.*, 1997] located in the payload bay, which recorded the energy spectrum of the ions returning to the Shuttle. With the TSS satellite deployed vertically upward, the EMF induced by eastward motion of the Orbiter in a southward Earth's magnetic field ((**v** x **B**) • **L** as shown in Fig. 1) results in a positively charged satellite, thus enabling it to collect electrons from ambient plasma. Take the last data point in the last stepping sequence of the third IV-24 cycle as an example (see Fig. 4). With Orbiter traveling at ~ 7.8 km/s, tether length of ~ 19.5 km, and the magnetic strength of ~ 0.4 gausses, the measured potentials distributed in the TSS circuit are: Ve = 3479.7 Volts, Vg =1866.3 Volts, and Vo < 10 Volts. The measured tether current is I = 0.375 Amperes. Using a mean tether resistance of 1821.4 Ω calculated specifically for this IV sequence, the satellite potential would be Vs = 930.4 Volts.

Each current pulse in the IV-24 cycle provides a set of values for I, Vg, Vo, and Ve. Using the Vs dataset obtained from the ROPE measurements, we can calculate the tether resistance R directly from (1). Figure 2 shows the R values for the first, second, and third IV-24 cycles as represented by the solid circle, square, and rhombic data points, correspondingly. Each data point is associated with a current pulse that gives rise to a satellite potential in the range of 1 Volt < Vs < 100 Volts. Adjacent data points are linked by a straight line. From this figure, we can see that for a given IV-24 cycle, the tether resistance data points form a distribution, which can be quantified statistically by a standard deviation around a mean value. Table 1 shows the mean and the standard deviation of the tether resistance (in Ω) averaged over each IV-24 cycle:

This table reveals an interesting fact: the mean tether resistance varies from cycle to cycle. Its value reaches the highest level in the first IV-24, then drops to the lowest level in the second IV-24 and, and finally settles at an intermediate value in the third IV-24. This variation is obviously correlated with the diurnal pattern of the three cycles. It is therefore logical to attribute the tether resistance variations to the temperature changes in the tether, which are directly influenced by exposure to sunlight. Since there is no direct temperature measurement of the tether, we look for variations in the temperature data taken by sensors attached to the skin of the satellite as corroborative evidence. Figure 3 displays temperature data (in °C) versus time from 16 sensors, which are part of the satellite thermal control system, located at various places on the surface of the satellite. The IV-24 periods are highlighted with heavy lines beneath the time axis. From this figure, we can see small periodic oscillations on the temperature curves at a period of roughly 4 minutes. These oscillations correspond to satellite spin at a rate of 0.25 rpm [*Stone and Bonifazi*, 1997]. A major temperature decline occurs at around 057/00:00 UT, which is the time the TSS enters the night orbit. From the first IV-24 to the second IV-24, the temperature decrease recorded by these sensors ranges from 10° C to 50° C, depending on where the sensor is located. Likewise, from the second IV-24 to the third IV-24, the temperature increases by similar amounts.

We can independently verify the temperature change based on the variation of mean resistance. The analytic temperature-

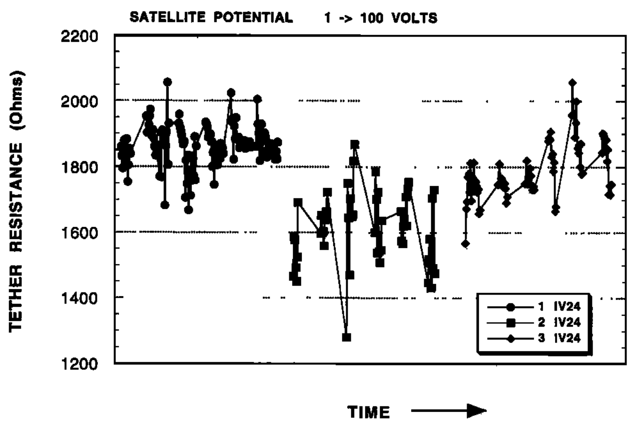

Figure 2. Tether resistance values derived from equation (1) based on ROPE measured Vs (< 100 Volts). Solid dots, squares, and rhombus are data points from the first, the second, and the third IV-24 cycle, respectively.

Table 1. Tether resistance calibration for the three IV-24 cycles

IV-24 Cycle	Orbit	Time (UT)	Mean Resistance	Standard Deviation
1st	Day	056/23:20:30 - /23:44:30	1864.2 Ω	60.2 Ω
2nd	Night	057/00:12:00 - /00:36:00	1610.0 Ω	109.5 Ω
3rd	Day	057/01:06:00 - /01:30:00	1788.4 Ω	84.3 Ω

resistance formula for copper is given in the Handbook of Chemistry and Physics [1980]

$$R = R_0 [1 + \Theta (T - T_0)] \quad , \qquad (2)$$

where T_0 = 20°C, R_0 = 2.0 KΩ, and Θ =0.00393 /°C. This formula relates the change of resistance to the change of temperature as

$$\Delta R = R_0 \, \Theta \, \Delta T \qquad (3)$$

Using the changes of mean resistance ΔR_1 (from 1st to 2nd IV-24) and ΔR_2 (from 2nd to 3rd IV-24) in Eq. (3), we can estimate the temperature change to be ΔT_1 = - 32° C and ΔT_2 = + 23°C. These numbers are in line with the temperature changes shown in Fig. 3. It is interesting to point out another feature that indicates temperature dependent resistance change of the TSS system. In Fig. 2, data points of the last IV-24 cycle show a slanted distribution in contrast to the first two cycles. This implies that the tether resistance increases with time during the last cycle. In Fig. 3, the satellite temperature measurements made at the last IV-24 show a similar trend of increase in time. This provides added evidence that the tether resistance is indeed sensitive to the temperature change.

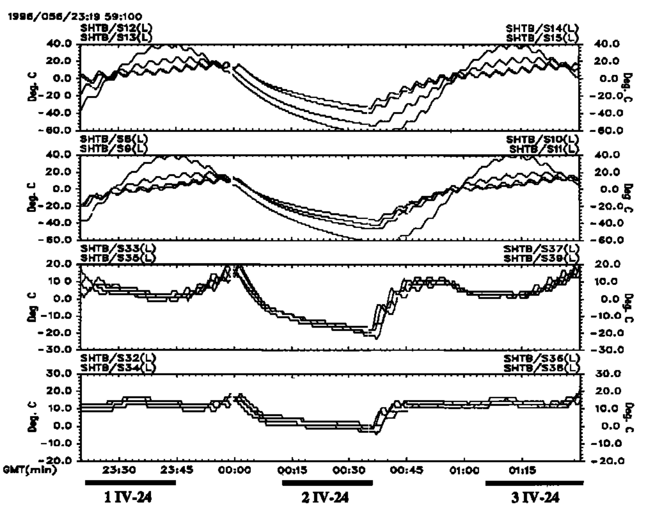

Figure 3. Temperature data from 16 sensors located on the satellite surface are plotted as functions of time. Dark broad lines below the time axis indicate the periods of three IV-24 cycles.

I-V Characteristics of the TSS Satellite

Using the calibrated tether resistance in Table 1, we can construct the entire I-V curve from Eq. (1). However, since the tether resistance varies with time during the TSS-1R mission, and can only be determined with some uncertainty, it is appropriate to impose error bounds on the I-V characteristics to indicate its limits. As an example, in Fig. 4 we plot the I-V curve obtained from the last stepping sequence of the third IV-24 cycle. This IV-24 cycle was performed during daytime, at high ambient plasma density (~ 8.2 x 10**5 /c.c. from real-time SUNDIAL model) [*Szuszczewicz et al.*, 1996], and with the tether near its full extension. In this figure, the tether current I for the entire current pulse sequence is plotted against the satellite potential, which is calculated from (1) based on the directly measured Ve and Vg from DCORE. Each current pulse contributes two data points, as shown by solid dots, and adjacent data points are connected by a straight line. The error bounds are imposed on voltage as horizontal bars because of the uncertainty on the measured tether resistance value. The actual length of the error bar is calculated by multiplying the tether current I with the standard deviation ΔR. As comparison, the Parker-Murphy I-V points obtained from the formula [*Parker and Murphy*, 1967]

$$(I / I^*) = 1+2 \, (Vs / V^*)^{1/2} \qquad (4)$$

are also plotted in this figure (represented by squares), where V* = 114 Volts for TSS and I* is the ambient thermal current collected by the resting satellite with no potential (I=I* as Vs=0). In calculating I*, the along-track TSS-1R electron density and temperature obtained by Szuszczewicz et al. [1997] are used. It is interesting to see that the TSS I-V curve exhibits distinctly different scaling properties at low and at high voltages. At high voltage (Vs > 50 Volts), the TSS I-V scaling seems to follow that of the Parker-Murphy model (i.e. I ~ $V^{1/2}$) as pointed out in a companion paper by Thompson et al. [1997]. At low voltage (Vs < 10 Volts), the TSS I-V curve deviates from the $V^{1/2}$ scaling, implying a shift in the physical processes involved in the current collection. Such distinct transition is typical in all of the third IV-24 sequences that involve high satellite potentials. It is also consistent with the observations that the ram ions are reflected when the satellite potential exceeds 5 Volts, which may cause significant modification on the plasma conditions surrounding the satellite at the transition [*Wright et al.*, 1997; *Winningham et al.*, 1997]. The possibility of a foreshock region upstream of the satellite created by the reflected ram ions which causes intense electron heating are currently being studied by the TSS-1R team [*Papadopoulos et al.*, 1997].

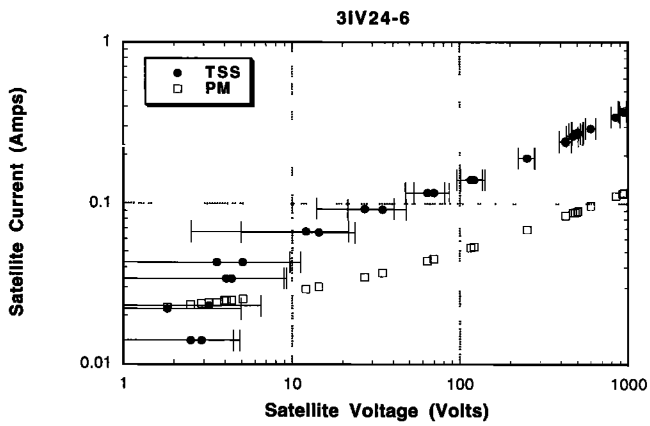

Figure 4. Typical I-V characteristics at high plasma density at the last stepping sequence of the 3rd IV-24 cycle. Error bars on satellite potential are due to the uncertainties of the resistance measurement.

Summary

We conducted a detailed calibration of the tether resistance by using the satellite potential measurements performed by the ROPE investigation in the TSS-1R mission. An important finding is that the tether resistance varies along the TSS orbit, as shown by Table 1. This variation correlates closely with the temperature changes of the TSS system. In addition, the tether resistance can only be determined with uncertainty. The uncertainty on tether resistance is reflected in the I-V characteristics of the TSS satellite because the resistance is an integrated part of the tether circuit. We constructed the I-V characteristics and imposed error bounds on the voltage value. The I-V curve exhibits distinctly different scalings at low (< 10 Volts) and high voltage regimes, which suggests fundamental changes in the physics and/or plasma conditions directly contributing to the current collection by the TSS satellite in the F region of the ionosphere.

Acknowledgment. This work was supported by NASA under contract NAS8-36811 and by ESA. We would like to acknowledge the contributions from the entire science team in the TSS-1R mission. We would also like to thank the crew members onboard STS-75 Drs. J. A. Hoffman, F. R. Chang-Diaz, C. Nicollier, U. Guidoni, M. Cheli, Lt. Col. S. J. Horowitz, and Lt. Col. A. M. Allen for their dedication to the mission and for their participation in performing the science investigations.

References

Aguero, V., P.M. Banks, B. Gilchrist, I. Linscott, W.J. Raitt, D. Thompson, V. Tolat, A.B. White, S. Williams, and P.R. Williamson, The Shuttle Electrodynamic Tether System (SETS) on TSS-1, *IL Nuovo Cimento*, 17, 49, 1994.

Bonifazi, C., F. Svelto, and J. Sabbagh, TSS Core Equipment. I. - Electrodynamic Package and Rationale for System Electrodynamic Analysis, *Il Nuovo Cimento*, 17, 13, 1994.

Burke, W.J., C. Bonifazi, D.A. Hardy, J.S. Machuzak, L.C. Gentile, D.G. Olson, C.Y. Huang, B.E. Gilchrist, J.-P. Lebreton, and C.A. Gurgiolo, Shuttle Charging during EGA Beam Emissions of TSS-1R, *Geophys. Rev. Lett.*, this issue, 1997.

Dobrowolny, M., and N.H. Stone, A Technical Overview of the TSS-1: the First Tethered-Satellite System Mission, *IL Nuovo Cimento*, 17, 1, 1994.

Handbook of Chemistry and Physics, Properties of Metals as Conductors, E85, 60th Ed., (1980).

Oberhardt, M.R., D.A. Hardy, W.E. Slutter, J.O. McGarity, D.J. Sperry, A.W. Everest III, A.C. Huber, J.A. Pantazis, and M.P. Gough, The Shuttle Potential and Return Electron Experiment (SPREE), *Il Nuovo Cimento*, 17, 67, 1994.

Papadopoulos, K., C.L. Chang, and A.T. Drobot, Ion Reflection by the TSS-1R Satellite, *Geophys. Res. Lett.*, this issue, 1997.

Parker, L.W., and B.L. Murphy, Potential Buildup on an Electron-Emitting Ionospheric Satellite, *J. Geophys. Res.*, 72, 1631, 1967.

Stone, N.H., K.H. Wright Jr., J.D. Winningham, J. Biard, and C. Gurgiolo, A Technical Description of the TSS-1 ROPE Investigation, *Il Nuovo Cimento*, 17, 85, 1994.

Stone, N.H., and C. Bonifazi, The TSS-1R Mission: Overview and Scientific Context, *Geophys. Res. Lett.*, this issue, 1997.

Szuszczewicz, E. P., P. E. Blanchard, P. Wilkinson, G. Crowley, T. Fuller-Rowell, P. Richards, M. Abdu, T. Bullett, R. Hanbaba, J.P. Lebreton, M. Lester, M. Lockwood, G. Millward, M. Wild, S. Pulinets, B.M. Reddy, I. Stanislawska, G. Vannaroni, and B. Zolesi, The First Real-Time Worldwide Ionospheric Predictions Network: TSS-1R Support Operations, *Geophys. Rev. Lett.*, this issue, 1997.

Thompson, D.C., C. Bonifazi, B.E. Gilchrist, S.D. Williams, W.J. Raitt, J.-P. Lebreton, and W.J. Burke, The Current-Voltage Characteristics of a Large Probe in Low Earth Orbit: TSS-1R Results, *Geophys. Rev. Lett.*, this issue, 1997.

Wright, K.H. Jr., N.H. Stone, J. Sorensen, J.D. Winningham, and C. Gurgiolo, Observations of Reflected Ions and Plasma Turbulence for Satellite Potentials Greater than the Ion Ram Energy, *Geophys. Res. Lett.*, this issue, 1997.

Winningham, J.D., N.H. Stone, C.A. Gurgiolo, K.H. Wright, R.A. Frahm, jand C.A. Bonifazi, Suprathermal Electrons Observed on the TSS1-R Satellite, , *Geophys. Res. Lett.*, this issue, 1997.

C.L. Chang, A.T. Drobot, and K. Papadopoulos, Applied Physics Operation, Science Applications International Corporation, McLean, Virginia. 22102

K.H. Wright, CSPAR, University of Alabama in Huntsville, Huntsville, Alabama 35899.

N.H. Stone, Space Science Laboratory, NASA/Marshall Space Flight Center, Huntsville, Alabama. 35812

C. Gurgiolo, Bitterroot Basic Research Inc., Hamilton, Montana. 59840

J.D. Winningham, Space Instrument Division, Southwest Research Institute, San Antonio, Texas 78228

C. Bonifazi, Agenzia Spaziale Italiana, Rome, Italy

(Received: January14, 1997; Revised: September 26, 1997; Accepted: October 15, 1997)